Quart. J. R. Met. Soc. (1980), **106**, pp. 581–598

551.574.12

The influence of entrainment on the evolution of cloud droplet spectra: I. A model of inhomogeneous mixing

By M. B. BAKER and R. G. CORBIN and J. LATHAM

Civil Engineering Dept., University of Washington, Seattle, USA

Physics Dept., UMIST, Manchester, England

(Received June 1979; revised 31 January 1980)

SUMMARY

In this, the first of two related papers, we present calculations of the growth of a population of condensate droplets rising above cloud base within small cumuli which are entraining undersaturated environmental air. It is assumed, on the basis of dimensional arguments and laboratory experiments on entrainment, conducted within a cloud droplet evolution tunnel, that this mixing process is inhomogeneous.

In the extreme situation to which the calculations apply undersaturated air is entrained in a stream, or in blobs, and some droplets of all sizes are completely removed from the condensate spectrum by evaporation, while others do not change in size. This is equivalent to assuming that the time constant for turbulent mixing (τ_T) is large relative to that for droplet evaporation (τ_r), and is thus the antithesis to the homogeneous model utilized by other workers, which assumes implicitly that $\tau_T/\tau_r = 0$.

The calculations based on the extreme inhomogeneous model produce spectral shapes which agree well with those reported in cumulus by Warner (1969a) and indicate that a small proportion of the droplets can grow several times faster through the condensate spectrum than classical theory predicts.

1. INTRODUCTION: THE CONCEPT OF INHOMOGENEOUS MIXING

This is the first of two papers concerned with the influence of entrainment of undersaturated environmental air upon droplet evolution in clouds. We designate them I and II. I introduces the concept, based upon laboratory experiments and simple theoretical arguments, of mixing as a non-classical, inhomogeneous process in which some droplets – of all sizes – are much more influenced by entrainment than others in their vicinity. This leads to some calculations of spectral evolution on both the classical and a limiting inhomogeneous model, which are designed to reveal the major differences between these two descriptions of entrainment. Existing observational evidence is then compared with predictions of both models. An outline of this work has been presented by Baker and Latham (1979). In II we present a description of a series of field studies of the influence of entrainment upon the water properties of clouds enveloping the UMIST field research station on the summit of Great Dun Fell, Cumbria. These are analysed in terms of the classical and inhomogeneous descriptions of entrainment, and provide support for the latter.

The evolution of droplet populations formed by condensation in natural clouds has been studied, experimentally and theoretically by many workers. The most detailed and reliable information on cumulus clouds of moderate depth has been provided by the airborne investigations conducted, presented and discussed by Warner (1969a, b, 1970, 1973a, b).

In these papers Warner points to important interrelated features of the shape and development of the droplet spectrum – prior to the onset of a significant contribution from coalescence – which he is unable to explain quantitatively. These are that (1) droplets of the smallest detectable size (diameter $d \sim 5\,\mu$m) are found at all levels within the clouds, irrespective of the distance from the vertical boundaries: (2) the droplet spectrum is consequently broad, and is commonly found to be bimodal: (3) the dispersion of the spectrum – defined as the ratio of the standard deviation to the mean diameter – is typically around 0·2 near the cloud base, and increases at higher levels. A further problem, which we believe may be closely related, is that the measured times required to produce raindrops in water clouds

may be appreciably shorter than values calculated on the classical theory of growth by condensation followed by stochastic coalescence. Various explanations (electric forces, velocity shear (Jonas and Goldsmith 1972), giant hygroscopic nuclei) have been advanced, but the problem cannot be regarded as resolved.

Warner (1969b) showed that the spectral shape and dispersion near cloud base can be explained if account is taken of the fact that the condensation coefficient for water vapour molecules is considerably below 1. His papers provide convincing evidence for the association of the other spectral features alluded to with mixing between the cloud and undersaturated environmental air. However, detailed calculations (Warner 1973a) in which entrainment of undersaturated environmental air was considered, yielded evolving spectra which, although they broadened with increasing altitude were quite unlike those observed. This led him to conclude that 'simple mixing between the cloud and the environment is unimportant in determining the droplet size distribution, at least in the early stages of cloud growth'.

On the other hand, Mason and Jonas (1974) and Jonas and Mason (1974) have presented calculations, based on a multi-thermal model of the air flow, from which they conclude that the major features of the droplet spectra can be explained in terms of mixing between the cloud and its environment. This conclusion has been challenged by Warner (1975) who argued that the dynamics, thermodynamics and microphysics employed in this treatment are unrealistic. The calculations have been defended by Mason (1975), but it is clear that no concensus of agreement exists as to the reasons for the particular features of cloud droplet spectra to which Warner has drawn our attention.

A recent contribution to this problem has been made by Lee and Pruppacher (1977). Essentially, they followed the theoretical approach to the mixing problem employed by Warner (1973a), but took account of the fact that aerosol particles active as cloud condensation nuclei are likely to be of mixed composition. Warner had considered a nucleus spectrum consisting exclusively of NaCl particles. Specifically, Lee and Pruppacher performed calculations for a 'maritime' aerosol, consisting of a mixture of NaCl and $(NH_4)_2SO_4$ particles, and a 'continental' aerosol in which the particles followed a Junge power law and each one was composed of 70% $(NH_4)_2SO_4$ and 30% of a water-insoluble material (a silicate). When entrainment of air and aerosol particles was considered broad spectra which developed double maxima were found, which were closer to reality than those predicted by other workers. Even so, substantial departures from Warner's field observations existed; in particular, the calculations seriously underestimate the rate of emergence of the second (smaller diameter) peak in the spectrum.

It seems reasonable to conclude that the role of entrainment in the evolution of droplet spectra is of major importance but that probably it has not been treated in a completely realistic manner.

We mention here a point developed in detail later: that in all the calculations alluded to the mixing process has been assumed to be *homogeneous*. In other words, the assumption has been made that all droplets at a given level in the cloud are, at any time, exposed to identical conditions of supersaturation or undersaturation. We have called this the classical description.

Laboratory experiments performed by Latham and Reed (1977), in which spectral changes were examined as undersaturated air was entrained into a slowly moving population of cloud droplets, yielded an alternative description of the mixing process which is central to the research described here. It is that the intermingling of cloudy and environmental air is a highly inhomogeneous process, with those droplets immediately adjacent to the infiltrating filaments, or blobs of undersaturated air being drastically affected, while those more remote being less so, or even unaffected. Subsequent mixing will thus produce a

broadening of the spectrum. This hypothesis appears, in principle, to have three favourable attributes: it associates the major spectral properties with a single process – entrainment, which is known to be important; it provides a mechanism for producing inhomogeneities in supersaturation which are not intimately tied to changes in updraught speed – thus circumventing the major obstacle to spectral broadening isolated by Bartlett and Jonas (1972); and it provides a mechanism for the more rapid growth by vapour diffusion of some fraction of droplets in the condensate spectrum. This third point is developed in more detail subsequently.

If the laboratory experiments of Latham and Reed have relevance to cloud physics it may be expected that adjacent regions would sometimes occur, within natural clouds, which possess closely similar droplet size distributions even when the values of liquid water content are very different. Knollenberg (1976) presented a pair of droplet spectra measured a few metres apart near cloud base which appear to lend support to this argument. The mode-diameter is more or less the same but one spectrum contains more than twice as many droplets as the other. He states (private communication) that such observations are common. Corbin *et al.* (1977), in a note concerned with inhomogeneities in natural clouds and fogs at Great Dun Fell, provide evidence for closely separated regions of widely different water content and essentially constant dispersion. Similar findings have been reported by Rodi (1978). More confirmatory evidence is presented in paper II.

2. Inhomogeneous mixing and laboratory experiments

Despite the support provided by the laboratory experiments of Latham and Reed (1977) the foregoing description of the mixing process is clearly simplistic. The extent to which it may be acceptable will depend upon certain rate processes associated with the mixing process within cumulus clouds. These are turbulent diffusion of the entrained air into the cloud; molecular diffusion at the interface between a blob and the surrounding cloudy air, and the evaporation of a droplet of radius r in an undersaturated environment. The characteristic times governing these three processes are defined as τ_T, τ_D and τ_r respectively. If τ_T or τ_D are much less than τ_r any inhomogeneities created by the mixing process will be substantially smoothed out before significant droplet evaporation can occur, and the mixing will approach the classical description employed by other workers. On the other hand, if $\tau_r \ll \tau_T, \tau_D$, the mixing process will approximate to the inhomogeneous description suggested by the experiments of Latham and Reed.

Taking X as the size of the blob, ε the rate of kinetic energy dissipation via turbulent mixing, D the molecular diffusion coefficient, $S(\%)$ the supersaturation, $\alpha(\sim 5\,\mu\text{m})$ the length associated with the condensation coefficient (Fukuta and Walter 1970), and characteristic values of the other parameters involved, we may write

$$\tau_T \sim (X^2/\varepsilon)^{\frac{1}{3}} \quad . \quad . \quad . \quad . \quad . \quad (1)$$

$$\tau_D \sim X^2/D \quad . \quad . \quad . \quad . \quad . \quad . \quad (2)$$

$$\tau_r \sim 10^{-6}(\rho_w/\rho_\infty)\{(r+\alpha)^2-\alpha^2\}/DS, \quad . \quad . \quad (3)$$

where r is measured in micrometres and ρ_w/ρ_∞ ($\sim 10^5$) is the ratio of the densities of liquid water and saturated vapour.

Taking $\varepsilon \sim 100\,\text{cm}^2\,\text{s}^{-3}$, $D \sim 0{\cdot}25\,\text{cm}^2\,\text{s}^{-1}$ we find that $\tau_T < \tau_D$ for all scales of interest. Thus the nature of the mixing will depend upon the relative values of τ_T and τ_r. If $\tau_T \gg \tau_r$ the evaporation will be essentially classical, whereas if $\tau_T \ll \tau_r$ the mixing process is slow and the picture approaches the limiting inhomogeneous one in which some droplets of all sizes are completely evaporated and the others are unaffected. Table 1 presents values of

TABLE 1. VALUES OF THE CRITICAL DISTANCE X_c (cm) PREDICTED FROM EQS. (1) AND (3) FOR VARIOUS VALUES OF DROPLET RADIUS (r), SUPERSATURATION (S) AND RATE OF KINETIC ENERGY DISSIPATION (ε)

	$S = -20\%$			$S = -5\%$		
r (μm)	$\varepsilon = 1$ (cm^2 s^{-3})	$\varepsilon = 10$ (cm^2 s^{-3})	$\varepsilon = 100$ (cm^2 s^{-3})	$\varepsilon = 1$ (cm^2 s^{-3})	$\varepsilon = 10$ (cm^2 s^{-3})	$\varepsilon = 100$ (cm^2 s^{-3})
1	0·1	0·3	1·0	0·8	2·6	8·2
3	0·7	2·1	6·8	5·5	17	55
5	1·8	5·8	18	15	46	147
10	8·0	25	80	64	200	640
15	21	65	210	175	550	1750
20	42	130	420	330	1050	3325

the critical scale-length X_c ($=\varepsilon^{\frac{1}{4}}\tau_r^{\frac{3}{2}}$, from (1) and (3)) for which $\tau_T/\tau_r = 1$, for various values of r, S and ε. It is seen that except for the highest levels of turbulence combined with low undersaturations the evaporation may be non-classical for scales in excess of about one metre.

The validity of these dimensional arguments was examined by performing mixing experiments in a specially constructed vertical wind tunnel. The basic system is illustrated in Fig. 1. In essence, a cloud of droplets was drawn up the tunnel (we call this the secondary stream), a flow of undersaturated air (the primary stream) was introduced into it from a nozzle located on the axis, and the droplet characteristics, temperature and flow speed were measured at many radial and axial positions above the nozzle. These experiments, with associated checks and procedures, are described in detail by Corbin (1979), and only the salient features are reproduced herein.

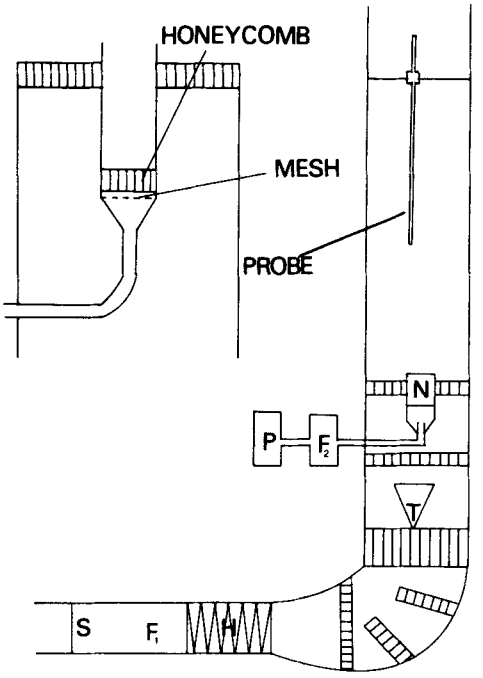

Figure 1. Schematic diagram of the experimental arrangement with (top left) detail of the larger (10 cm) mixing nozzle. S is the shutter, F_1 the fan, H the humidifier, T the spinning top, N the nozzle, F_2 the flow-meter and P the pump. The hatched areas represent honeycombing.

A spinning-top generator (May 1949), mounted axially in the vertical section of the tunnel, about 1 m below the test section, was used to produce a unimodal droplet cloud covering the radius range 6 to 15 μm. In acceptable conditions the droplet spectrum did not alter significantly with height or time during the course of an experiment (about 40 minutes). The drop sizes and concentrations were measured using an electrostatic disdrometer (Keily probe, Corbin *et al.* 1978). This was specially calibrated for an orifice diameter of 100 μm and wind speed 0·3 m s^{-1}.

Two mixing nozzles were used in the experiments. The larger one was of diameter 10 cm, and the smaller one 3·8 cm. The former is illustrated in the insert to Fig. 1. The temperature in the mixing region was measured using a miniature bead thermistor, and a hot-wire anemometer was built to measure the wind velocity and turbulent characteristics. The turbulent intensity defined as the ratio $U'/\bar{U}$ of the root mean square of the velocity fluctuations to the mean velocity was typically around 0·02 in the absence of drops.

In the 19 acceptable experiments that were performed measurements were made with both the large and the small nozzles (Table 2). The airspeed along the tunnel (U), the flowrate in the primary stream (F), the temperatures (T_1 and T_2) in the primary and secondary streams, and the relative humidity (H) in the primary stream ranged respectively from 10 to 36 cm s^{-1}, 7 to 300 litres per minute, 18·5 to 33·5°C, 17·5 to 23°C, and 40 to 100%. Studies were made also with no primary stream ($F = 0$).

Table 2 shows that in all runs with the smaller nozzle the final mean radius of the droplets in the cloud was significantly lower, after entrainment, than the initial radius. On the other hand, no significant change in size was found in nearly all of the runs with the larger nozzle although the rate of arrival of droplets at the Keily probe was substantially reduced, suggesting that the liquid water content was appreciably diminished. As a check on this latter point direct measurements of the liquid water content before and after mixing

TABLE 2. PARAMETER VALUES AND RESULTS FOR 19 ENTRAINMENT EXPERIMENTS. S AND L REFER TO SMALL OR LARGE NOZZLE RESPECTIVELY. U IS THE AIR SPEED ALONG THE WIND TUNNEL, F THE FLOWRATE IN THE PRIMARY STREAM, T_1 AND T_2 THE TEMPERATURES IN THE PRIMARY AND SECONDARY STREAMS AND H THE RELATIVE HUMIDITY IN THE PRIMARY STREAM. r_i AND r_f ARE THE INITIAL AND FINAL MEAN RADII; IN RUNS 1, 2, 3, 11 AND 12 THESE ARE THE AVERAGE RADII ($\Sigma nr/\Sigma n$) AND IN THE REMAINING RUNS THEY ARE THE VOLUME MEAN RADII ($\Sigma nr^3/\Sigma n)^{\frac{1}{3}}$. THE FRACTIONAL REDUCTION IN LIQUID WATER CONTENT, f, WAS MEASURED DIRECTLY IN ONLY 7 RUNS

Run	Nozzle	U (cm s^{-1})	F (l min^{-1})	T_1 (°C)	T_2 (°C)	H (%)	r_i (μm)	r_f (μm)	f (%)
1	S	34	50	23	21·5	53	7·8±0·3	6·3	
2	S	34	100	20	19	42	7·7±0·5	6·5	23
3	S	36	100	24	23	49	7·9±0·7	6·4	
4	L	36	100	21	23	52	9·8±0·4	9·6	
5	L	36	100	21	23	52	10·4±0·8	9·7	
6	L	35	100	33·5	20	100	8·7±0·4	9·2	
7	L	35	100	20	17·5	64	10·1±0·7	9·6	
8	L	14	65	18	18	60	10·0±0·6	10·5	
9	L	10	40	21·5	19	60	9·9±0·5	10·5	
10	L	10	100	21·5	19	60	10·3±0·7	10·3	30
11	S	10	7	19·5	18	55	9·6±0·5	7·7	
12	L	10	100	21	20	55	8·7±0·5	8·8	
13	L	10	50	19	19	55	11·5±0·5	11·2	18
14	L	10	100	19	19	55	11·5±0·5	11·0	33
15	L	10	150	19	19	55	11·5±0·5	11·1	48
16	L	10	200	19	19	55	11·5±0·5	11·4	62
17	L	10	300	19	19	55	11·5±0·5	11·0	87
18	L	10	100	18·5	18·5	40	10·6±0·5	10·4	
19	L	10	200	18·5	18·5	40	10·6±0·5	10·7	

were made in several runs. Values of the associated fractional reduction f in water content are given in the table. It is seen that they are considerable. Calculations of the expected reduction of water content agreed well with the measured values.

Figure 2 presents spectra measured on the axis of the tunnel ($R = 0$) at a distance $Z = 2{\cdot}3$ m above the large nozzle for various rates of flow F of the primary stream. It is seen that as F increases the liquid water content diminishes but the spectral shape and mean droplet size are preserved, to a first approximation. For this value of Z the water content and spectral shape are independent of R. Measurements made at smaller values of Z illustrate the slow lateral mixing of the droplets into the axial regions – with constant spectral shape – as the cloud ascends the tunnel.

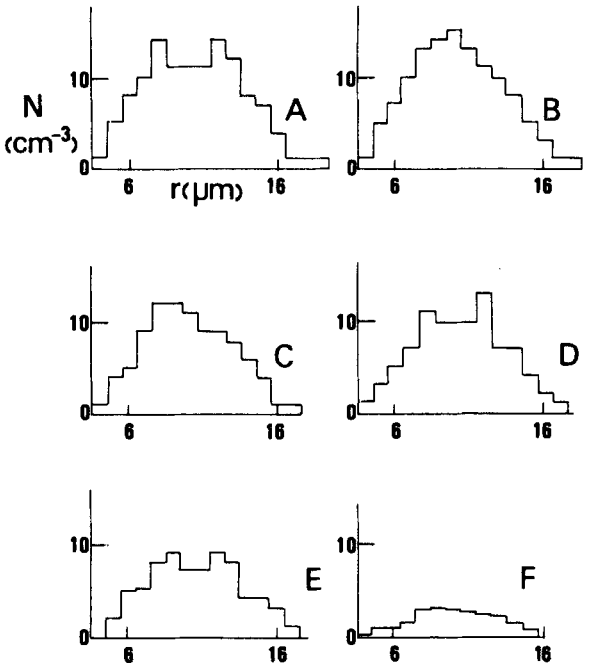

Figure 2. Droplet size distributions measured at $z = 2{\cdot}3$ m in runs 13 to 17 with various primary flow rates F (plus one run with $F=0$). Large nozzle. n is the number of droplets in each histogram.

Histogram	A	B	C	D	E	F
F (1 min^{-1})	0	50	100	150	200	300
n	3639	3727	3016	2885	2181	1478

Statistical examination of the measured time intervals between successive droplets arriving at the Keily probe was performed on a uniform cloud, in the absence of entrainment. It showed that the distribution of droplets was random. A similar analysis was performed in a number of runs in which entrainment occurred, in order to reveal evidence of any structure that might be present in the cloud, especially in the mixing region. A simple mathematical treatment of this problem shows that the number of droplets N arriving at the Keily probe within a time interval τ following their immediate predecessors is related to the average rate of arrivals, α, by

$$\log N = -\alpha\tau + A,$$

where A is a constant, of specifiable value for a given cloud. Thus, if $\log N$ is plotted against

τ any non-randomness in the distribution of droplets in the cloud under study should show up as a non-linear relationship. Such as interarrival time analysis was performed on recordings of Keily probe pulses in a number of runs. A typical example, obtained for run 10, is presented in Fig. 3, where $(\log N)/\tau$ histograms are shown for a small number of the distances Z at which results were obtained. They illustrate the evolution from a random distribution prior to mixing (A) to a cloud with considerable structure (B) at $Z = 20$ cm – which appears to correspond to pockets of original cloud intermixed with regions of zero or low droplet density – followed (C to D) by gradual smoothing to an essentially homogeneous final state.

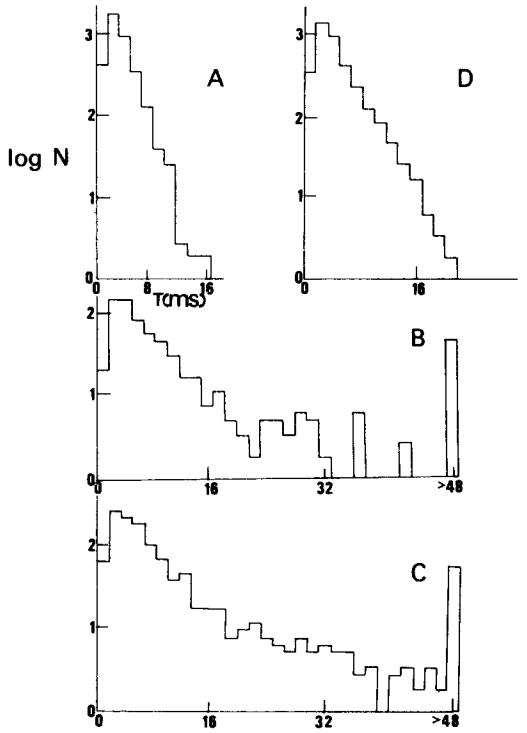

Figure 3. The measured distribution of intervals τ between the arrival of consecutive pulses at the Keily probe in run 10, with the large nozzle, at a radial distance $R = 13$ cm and various distances z above the nozzle. A, $z = 0$; B, $z = 20$ cm; C, $z = 40$ cm; D, $z = 100$ cm.

A more detailed description of experiments to examine structure in the water properties and to determine the spacings between successive eddies is given by Corbin (1979). This includes an account of attempts to use an imposed temperature difference between the primary and secondary streams as an indicator of the mixing process.

These experiments provide a test of the simple arguments, concerned with time constants, presented at the beginning of this section if (by utilizing both nozzles) the conditions $\tau_T/\tau_r < 1$ and $\tau_T/\tau_r > 1$ can be achieved. In the former case mixing will be rapid and the evaporation should approach the classical description; in the latter case it will be distinctly inhomogeneous. Corbin (1979) shows that values of eddy diffusivity can be obtained from the experimental results, and that these lead to values of $\tau_T \sim 6$ s for the larger nozzle and $\tau_T \sim 2$ s for the smaller. The values of τ_r for the conditions employed in the experiments

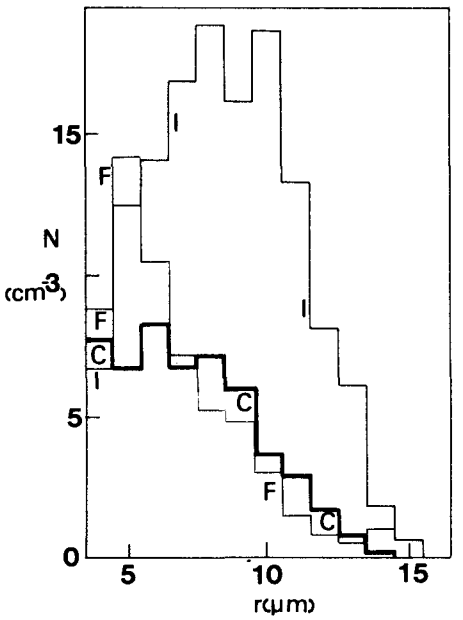

Figure 4. Droplet size distributions for run 2, with the small nozzle. *I*, before mixing; *F*, after mixing; *C*, predicted on the modified classical model of evaporation, described in the text.

were generally in the range 3 to 4 s, so experiments with the two nozzles may be expected to yield the required range of conditions.

The results presented are generally consistent with the foregoing arguments, and an attempt was made to assess their quantitative validity. Figure 4 presents the initial and final spectra measured in run 2 with the smaller nozzle, together with a calculated spectrum, based on the assumption (outlined above) that droplets embedded in saturated air and drawn into the primary stream at a rate given by the experimental measurements, all experienced identical values of H at a given level. The spectrum predicted by this modified classical model is seen to agree well with that measured. On a strictly classical model mixing would be instantaneous over the entire width of the tunnel and the spectral changes would bear no relation to those observed. In Fig. 5 we present initial and final spectra measured in run 13, with the larger nozzle. Within the experimental limitations the spectral shape and mean size are seen to be preserved, as is predicted by the preceding arguments, for $\tau_T/\tau_r > 1$.

It would have been desirable, in order to check the validity of the foregoing interpretation and establish directly whether the results were an artefact of the characteristics of the nozzles and the air-flow through them, to have performed further experiments with the larger nozzle in which much larger droplets were utilized. In this circumstance $\tau_r/\tau_T > 1$ and the results for the larger nozzle would be similar to those reported for the smaller one, if our dimensional arguments are correct. Unfortunately this test was not possible with our experimental arrangement, since the electrostatic disdrometer is not able to size droplets of the required larger size. However, it appears relevant to cite, in this connection, the more rudimentary experiments of Latham and Reed (1977), in which it was found that for similar nozzle sizes and flow rates to those employed in the present experiments no spectral changes accompanied the evaporative process when a cloud consisted of very small droplets

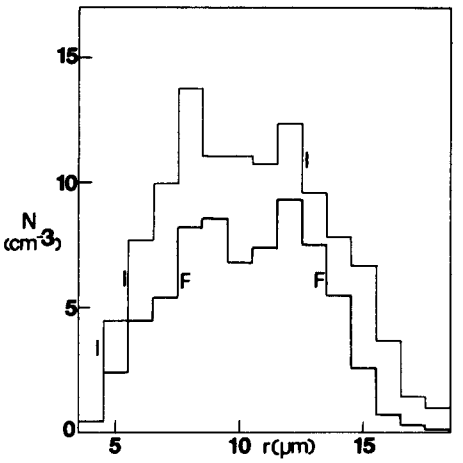

Figure 5. Droplet size distribution for run 15, with the large nozzle. *I*, before mixing; *F*, after mixing.

($r \sim 4\,\mu$m), whereas the peak radius was significantly reduced when larger ones ($r \sim 14\,\mu$m) were utilized.

We conclude that the present experiments provide support for the arguments presented earlier concerning the crucial role of the ratio τ_T/τ_r in affecting the droplet spectrum.

3. Computations of spectral evolution in clouds

In order to examine the influence on spectral evolution of the inhomogeneous mixing of undersaturated and cloudy air we have modelled the process by a simple mechanism which represents an extreme, or limiting, case corresponding to the condition $\tau_r/\tau_T \to 0$. In this model undersaturated blobs of volume v_0 and relative humidity H are entrained into an ascending parcel of cloud, of volume V, at a constant mean rate. The CCN spectrum in each blob is composed of NaCl particles in equilibrium at H. The mechanics of the encounter between a blob and the rising cloud are not specified but the result – based on the experiments of Latham and Reed, together with the foregoing dimensional arguments – is assumed to be the complete removal by evaporation of some droplets of all size categories with no discrimination as to size, the remaining droplets being unaffected by the infiltrating undersaturated air. This process of evaporation is assumed to occur on a time-scale short in comparison with that for turbulent mixing (i.e. $\tau_r/\tau_T \to 0$) and to continue until the relative humidity within the blob rises to 100%, at which stage the NaCl particles contained within it will have grown by condensation to their equilibrium values at this humidity. In the second stage of mixing the blob and the region affected by it are assumed to mix instantaneously with the surrounding cloudy air.

The physical situation to which this model of evaporation may be considered to correspond is as outlined in the Introduction. Undersaturated air is entrained into a cloud in the form of turbulent blobs or filaments. As those deform and infiltrate the cloud they produce sharp interfacial vapour gradients which result in the evaporation of those droplets in their immediate vicinity whilst exercising negligible influence upon those droplets remote from the interface. If the evaporation time is short compared with the turbulent mixing time ($\tau_r/\tau_T \ll 1$) the droplets at the interface will be completely evaporated whilst the

others will be unaffected.

The evolution of the cloud from time $t = 0$, relative humidity 100%, through the first 1000 seconds was computed for the following three cases:

(1) *Homogeneous entrainment* (H). This is the classical model (see, for example, Warner (1969b)), in which environmental air and nuclei are entrained at a constant rate

$$\mu = (1/V)\partial V/\partial t.$$

(2) *Adiabatic ascent* (A). There is no exchange with the environment.

(3) *Inhomogeneous entrainment* (I). Dry air and nuclei are entrained in discrete blobs of volume v_0 at a mean rate $\lambda(t)$.

In all the computations we assumed the environmental humidity H = constant = 80% and the environmental lapse rate $\Gamma = -7{\cdot}5°\mathrm{C\,km^{-1}}$. The updraught speed U was a constant and the cloud base temperature $T(o)$ was prescribed. The initial NaCl nucleus spectrum and the number of size classes included were based loosely on those employed by Warner (1969b) and Lee and Pruppacher (1977). The CCN activity spectrum in the air beneath cloud base was assumed identical to that in the entrained air (models H and I). The following equations, based on the original model of Warner (1969b) were used to describe the evolution of the cloud droplet spectrum:

Homogeneous case (H)

$$\frac{dV}{dt} = \mu V, \qquad (4)$$

$$\frac{dT}{dt} = -\left[A\left(1+\frac{B}{T}q_s\right)+\mu(T-T_{\mathrm{out}})+\frac{\mu\mathscr{L}}{\rho_{\mathrm{air}}c_p}\{\rho_s(T)(1+S/100)-H\rho_s(T_{\mathrm{out}})\}+\right.$$

$$\left.+\frac{\mu c_w LT}{c_p\rho_{\mathrm{air}}}\right]/(1+Cq_s/T^2), \qquad (5)$$

$$\frac{dS}{dt} = -\beta+\mu\{H-(S+100)\}-(S+100)\left(\frac{1}{\rho_s}\frac{d\rho_s}{dT}\frac{dT}{dt}+\frac{E}{T}\right), \qquad (6)$$

where $S(\%)$ is the supersaturation, β describes the consumption of water vapour by condensation on to the droplet population, $\rho_s(T)\,(\mathrm{g\,cm^{-3}})$ is the water vapour density at saturation at temperature T, $\rho_{\mathrm{air}}\,(\mathrm{g\,cm^{-3}})$ the density of air, $T(°\mathrm{K})$ and $T_{\mathrm{out}}(°\mathrm{K})$ the temperature inside and outside the cloud, and $q_s = \rho_s/\rho_{\mathrm{air}}$. c_p and $c_w\,(\mathrm{erg\,(g\,°K)^{-1}})$ are the specific heats at constant pressure of water vapour and condensed water respectively, and $\mathscr{L}(\mathrm{erg\,g^{-1}})$ is the latent heat of vaporization of water. A, B, C and E are taken to be constants. We took

$$\rho_{\mathrm{air}} = 1{\cdot}2\times10^{-3}\,\mathrm{g\,cm^{-3}}$$
$$c_w = 4{\cdot}2\times10^{7}\,\mathrm{erg\,(g\,°K)^{-1}}$$
$$c_p = 1\times10^{7}\,\mathrm{erg\,(g\,°K)^{-1}}$$
$$\mathscr{L} = 2{\cdot}5\times10^{10}\,\mathrm{erg\,g^{-1}}$$
$$A = 9{\cdot}78\times10^{-3}\,°\mathrm{K\,m^{-1}}$$
$$B = 8{\cdot}61\times10^{3}\,°\mathrm{K}$$
$$C = 1{\cdot}31\times10^{7}\,(°\mathrm{K})^2$$
$$E = 3{\cdot}42\times10^{-2}\,°\mathrm{K}.$$

Equations (4) to (6) must be supplemented by the defining equations for $\rho_s(T)$ and β. We have assumed

$$\rho_s(T)\,(\mathrm{g\,cm^{-3}}) = 1{\cdot}8\times10^{3}\exp(-5400/T) \qquad (7)$$

and $$\beta\ (\mathrm{s}^{-1}) = \frac{10^{-10}}{\rho_s} 4\pi \sum_{i=1}^{N} r_i^2\, n(r_i,t) \frac{dr_i}{dt}, \quad . \quad . \quad (8)$$

where N is the number of size classes and $n(r_i,t)\,(\mathrm{cm}^{-3})$ is the density of droplets of radius $r_i\,(\mu\mathrm{m})$. Furthermore, we took

$$\frac{dr_i}{dt}\,(\mu\mathrm{m\,s}^{-1}) = \frac{1{\cdot}0}{r_i+\alpha}\left[S - \frac{0{\cdot}115}{r_i} + \frac{1{\cdot}41\times10^{13}\, m_i}{r_i^3}\right] \quad . \quad . \quad (9)$$

Here α, the length scale associated with non-ideality in water condensation, was put equal to $5\,\mu$m. m_i (g) is the mass of the ith NaCl nucleus.

Adiabatic case (A). The equations for this case are Eq. (4)–(9) above, with $\mu = 0$.

Inhomogeneous case (I). The entrainment of discrete parcels of dry air is assumed to occur instantaneously, at times $t = t_i$. Then

$$\frac{dV}{dt} = v_0 \sum_i \delta(t-t_i), \quad . \quad . \quad . \quad (10)$$

where $\delta(x)$ is the Dirac delta function.

$$\frac{dT}{dt} = -\left[\left[A\left(1+\frac{B}{T}q_s\right) + \frac{v_0}{V}\sum_i \delta(t-t_i)\left[T - T_{\mathrm{out}} + \right.\right.\right.$$

$$\left.\left.\left. + \frac{\mathscr{L}}{\rho_{\mathrm{air}} c_p}\{\rho_s(T)(1+S/100) - \rho_s(T_{\mathrm{out}})H\} + \frac{c_w L T}{c_p \rho_{\mathrm{air}}}\right]\right]\right] \Big/ \left(1 + C\frac{q_s}{T^2}\right) \quad (11)$$

$$\frac{dS}{dt} = -\beta - (100+S)\left(\frac{1}{\rho_s}\frac{d\rho_s}{dT}\frac{dT}{dt} + \frac{E}{T}\right) - \frac{v_0}{V} S \sum_i \delta(t-t_i). \quad (12)$$

All parameters in this set of equations have their previously defined meanings and values. In this case the total number density of droplets, $n\,(\mathrm{cm}^{-3})$, is constant between blobs (when the evolution process is adiabatic). Each encounter of dry and moist air produces instantaneous evaporation of a given fraction F of the droplets in each size category. That is

$$\partial n(r_i,t)/\partial t\big|_{\mathrm{evaporation}} = -\sum \delta(t-t_i)\, n(r_i,t)\, F\,(1+v_0/V)^{-1}, \quad . \quad (13)$$

where F, the fraction of droplets evaporated, is given by

$$F = \frac{v_0}{LV}\{\rho_s(T) - H\rho_s(T_{\mathrm{out}})\} \quad . \quad . \quad . \quad (14)$$

The rate of change of the droplet density due to dilution by mixing is

$$\partial n(r_i,t)/\partial t\big|_{\mathrm{dilution}} = -\sum_i \delta(t-t_i)\, n(r_i,t)\,(v_0/V)(1+v_0/V)^{-1} \quad . \quad (15)$$

The entrainment rate is adjusted to keep $n\,(\mathrm{cm}^{-3})$, the total droplet number density, constant:

$$\partial n(r_i,t)/\partial t\big|_{\mathrm{entrainment}} = \sum_i \delta(t-t_i)\, n_0(r_i)\,(F + v_0/V)(1+v_0/V)^{-1}, \quad . \quad (16)$$

where $n_0(r_i)\,(\mathrm{cm}^{-3})$ is the (constant) density of dry nuclei of radius r_i in the environment. In the computations the mean entrainment rate was kept the same for cases (H) and (I), and the blob volume v_0 was varied from 0·01 to 0·1 times the original cloud volume $V(o)$. In order to avoid complications in interpretation resulting from variations in droplet concentration the CCN activity spectrum was chosen so that all entrained nuclei were activated during subsequent ascent.

A time step of one second and simple first order integration scheme were used for all equations except (9) for which we used a fourth-order Runge–Kutta algorithm with variable time step. In case (H), to save computation time, entrainment of dry particles was accounted for only every ten seconds. The output from these numerical experiments consisted of the computed droplet spectra, $S(t)$, $T(t)$ and $L(t)$, over the first 1000 seconds of cloud evolution. Calculations were made for: $U = 1, 2\,\mathrm{m\,s^{-1}}$; $T(o) = 278, 283, 288°\mathrm{K}$; $N = 100, 200, 300, 600\,\mathrm{cm^{-3}}$; $n = 6, 38$; and $\mu = 5\times10^{-4}, 10^{-3}\,\mathrm{m^{-1}}$.

We wish to emphasize that the primary objective of these calculations was to establish whether our extreme model of inhomogeneous mixing ($\mathrm{I}, \tau_r/\tau_T \to 0$) provides a more accurate description of the effect of entrainment upon cloud droplet evolution than the classical, homogeneous model (H), which can be regarded as the opposite extreme ($\tau_r/\tau_T \to \infty$). Accordingly, there was no justification for attempting to incorporate into our calculations a full treatment of the cloud dynamics. It appeared to us adequate to base our calculations upon the simple model of Warner (1969b) and to ensure that the average entrainment rates were identical in the homogeneous and inhomogeneous models – from which it follows that, to within a few percent, the liquid water contents at any level were the same on models H and I. This was found always to be so (Table 3). Thus, in the crude model employed in our calculations, entrainment – with associated evaporation and temperature changes – does not disturb the upward progression of the cloud parcel and no consideration is given to the route or mechanism by which the undersaturated air enters the cloud. The description of inhomogeneous evaporation employed (based on $\tau_r/\tau_T \to 0$) is extreme and optimal for producing enhanced growth rates of favoured droplets (discussed subsequently). An additional simplification was to prescribe, rather than calculate, the total amount of evaporation resulting from the entry of a blob into the cloud. A series of subsidiary calculations demonstrated that no significant errors resulted from this procedure. On the inhomogeneous model the frequency of ingestion of blobs was taken to be

$$\lambda = \mu U(V/v_0) \quad . \quad . \quad . \quad . \quad (17)$$

in the majority of calculations. An alternative expression

$$\lambda = \mu U(V_0/v_0) \quad . \quad . \quad . \quad . \quad (18)$$

was employed occasionally.

TABLE 3. CALCULATED VALUES, AT VARIOUS TIMES t, OF LIQUID WATER CONTENT (L), SUPERSATURATION (S), MAXIMUM DROP RADIUS (R) AND CONCENTRATION OF DROPLETS OF RADIUS R (N_T, INHOMOGENEOUS CASE ONLY). THE SUFFICES H, A AND I REFER RESPECTIVELY TO THE HOMOGENEOUS, ADIABATIC AND INHOMOGENEOUS MODELS. $1/\lambda_0 = 10\,\mathrm{s}$. CALCULATIONS ON THE HOMOGENEOUS MODEL WERE NOT MADE BEYOND 700 s

$t(s)$	100	200	300	400	500	600	700	800	900	1000
T_c(°C)	14·4	13·7	13·0	12·3	11·5	10·8	10·0	9·3	8·5	7·7
T_e(°C)	14·2	13·5	12·7	12·0	11·2	10·5	9·7	9·0	8·2	7·5
$R_H(\mu m)$	8·5	10·2	11·3	12·2	13·0	13·8	14·5	—	—	—
$R_A(\mu m)$	9·3	11·0	12·1	12·9	13·6	14·2	14·8	15·3	15·8	16·2
$R_I(\mu m)$	10·5	15·2	17·6	19·4	20·5	22·2	23·3	24·3	25·2	26·1
$N_T(1^{-1})$	58	6·3	2·6	1·4	0·57	0·53	0·36	0·26	0·19	0·15
$L_H(\mathrm{g\,m^{-3}})$	0·10	0·26	0·39	0·51	0·62	0·72	0·80	—	—	—
$L_A(\mathrm{g\,m^{-3}})$	0·20	0·46	0·71	0·94	1·18	1·41	1·64	1·86	2·09	2·31
$L_I(\mathrm{g\,m^{-3}})$	0·06	0·27	0·41	0·52	0·62	0·71	0·79	0·88	0·93	1·00
$S_H(\%)$	0·37	0·20	0·17	0·16	0·15	0·14	0·14	—	—	—
$S_A(\%)$	0·37	0·21	0·17	0·15	0·13	0·12	0·11	0·10	0·10	0·09
$S_I(\%)$	1·12	0·55	0·42	0·41	0·38	0·39	0·38	0·33	0·38	0·34

4. Results

It was reassuring to find that although computational economies limited us to a much smaller number of size classes in the CCN activity spectrum than was considered by Warner (1969b) our computed spectral evolution for the homogeneous case (H) agreed well with his for the same values of the other parameters.

The general evolution of the cloud droplet spectrum, as predicted by the inhomogeneous model when blobs of environmental air are entrained at an initial rate $\lambda_0^{-1} = 10\,\mathrm{s}$, is illustrated in Fig. 6. This frequency is the same as that used for the homogeneous case (H), so crudely we may regard the entrainment as occurring in a steady stream. It is seen that as the cloudy air rises the spectrum flattens and broadens and the dispersion γ (defined as the ratio of the standard deviation to the mean size) increases, in the manner reported by Warner (1969a) to be characteristic of non-precipitating cumuli.

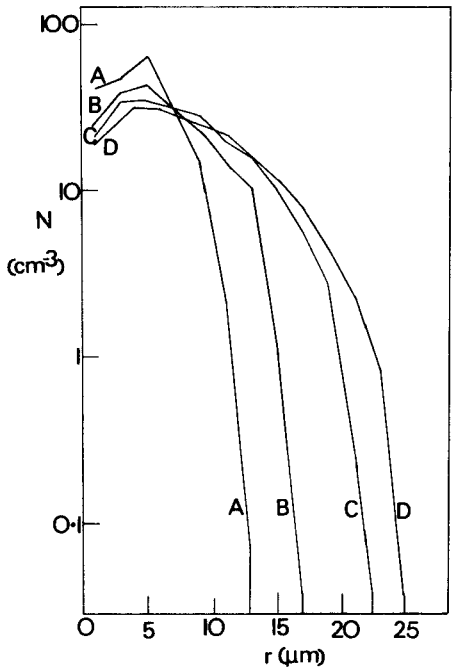

Figure 6. Predicted size distributions on the inhomogeneous model at various distances Z above cloud base. $U = 1\,\mathrm{m\,s^{-1}}$. $1/\lambda_0 = 10\,\mathrm{s}$. $T(o) = 15°\mathrm{C}$. $N = 200\,\mathrm{cm^{-3}}$. $n = 6$. $\mu = 10^{-3}\,\mathrm{m^{-1}}$. *A*, $Z = 150\,\mathrm{m}$; *B*, $Z = 350\,\mathrm{m}$; *C*, $Z = 650\,\mathrm{m}$; *D*, $Z = 1000\,\mathrm{m}$.

A more precise comparison of the predictions of our inhomogeneous model with the observations of Warner (1969a) is provided by Figs. 7 and 8, in each of which is presented a typical size distribution (*W*) measured by Warner, together with a predicted curve (*I*) for the same liquid water content, L, with $\lambda_0^{-1} = 10\,\mathrm{s}$. In the former case $L \sim 0{\cdot}4\,\mathrm{g\,m^{-3}}$ and in the latter $L \sim 0{\cdot}7\,\mathrm{g\,m^{-3}}$. The agreement between the observed and inhomogeneous curves is seen to be excellent in both cases – the deviations at the smallest droplet size possibly being due to experimental difficulties involved in sampling droplets of radius $r \sim 2\,\mu\mathrm{m}$ with the sooted-slide technique. On the other hand the curves (H), based on the classical, homogeneous description of entrainment, are similar to those calculated by

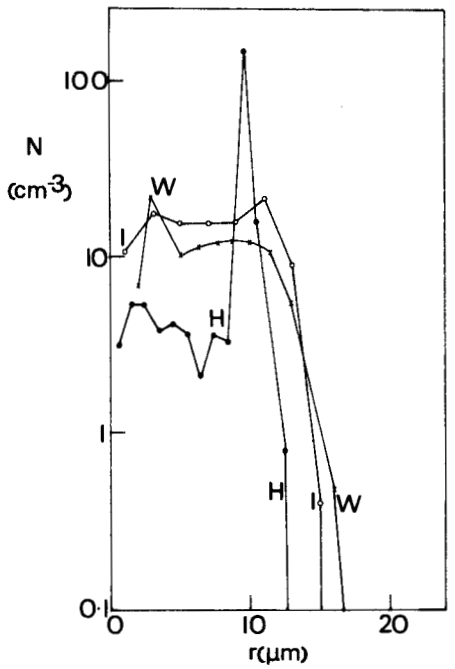

Figure 7. Droplet size distributions in cumulus: *W*, measured by Warner (1969a); *H*, calculated on the homogeneous model; *I*, calculated on the inhomogeneous model. $U = 1\,\mathrm{m\,s^{-1}}$, $1/\lambda_0 = 10\,\mathrm{s}$, $T(o) = 15°\mathrm{C}$, $N = 200\,\mathrm{cm^{-3}}$, $n = 6$, $\mu = 10^{-3}\,\mathrm{m^{-1}}$, $L = 0{\cdot}4\,\mathrm{g\,m^{-3}}$.

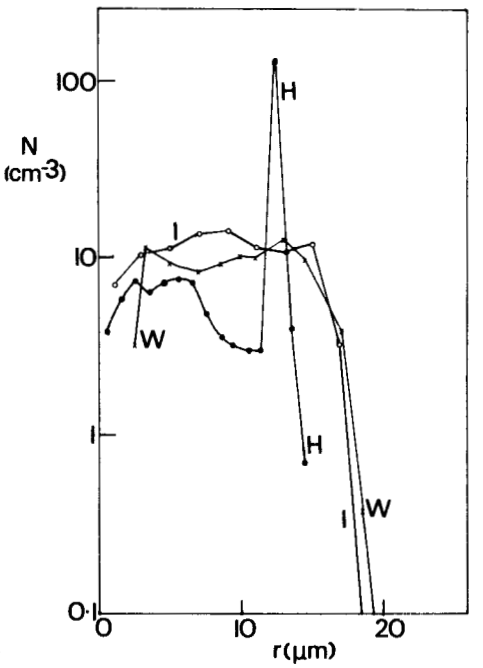

Figure 8. Droplet size distributions in cumulus: *W*, measured by Warner (1969a); *H*, calculated on the homogeneous model; *I*, calculated on the inhomogeneous model. $U = 1\,\mathrm{m\,s^{-1}}$, $1/\lambda_0 = 10\,\mathrm{s}$, $T(o) = 15°\mathrm{C}$, $N = 200\,\mathrm{cm^{-3}}$, $n = 6$, $\mu = 10^{-3}\,\mathrm{m^{-1}}$, $L = 0{\cdot}7\,\mathrm{g\,m^{-3}}$.

Warner, but bear little resemblance to those observed. The values of spectral dispersion calculated on the inhomogeneous model increased with altitude above cloud base and agreed well with those measured by Warner (1969a).

Another problem on which Warner has focused attention is the frequent occurrence of bimodal spectra in cumulus clouds. Spectra containing more than one mode are predicted by the inhomogeneous model when the frequency of infiltration of the cloud by blobs, λ, is low. An example of a bimodal spectrum produced by the model when $\lambda_0^{-1} = 200$ s is presented in Fig. 9. It is seen to resemble ones measured by Warner (1969a).

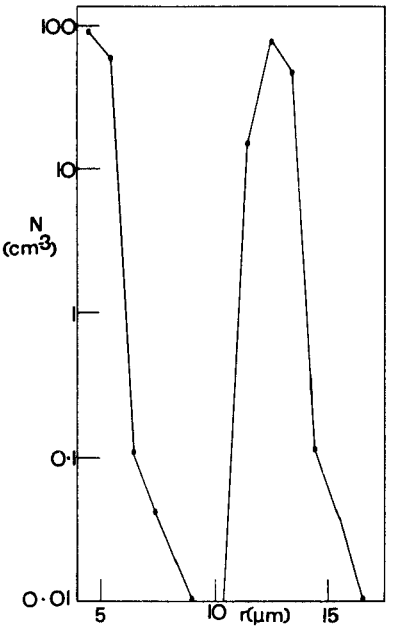

Figure 9. Bimodal spectrum produced on the inhomogeneous model. $N = 300\,\text{cm}^{-3}$; $n = 38$; $1/\lambda_0 = 200$ s; $L_I = 1{\cdot}9\,\text{g m}^{-3}$; $U = 1\,\text{m s}^{-1}$; $\mu = 5 \times 10^{-4}\,\text{m}^{-1}$.

Table 3 presents values of liquid water content L_H, L_A L_I, supersaturation S_H, S_A, S_I and maximum radius of droplets in the spectrum, R_H, R_A, R_I, after various growth times t for the homogeneous, adiabatic and inhomogeneous models ($\lambda_0^{-1} = 10$ s) respectively. Also presented are values of the concentration N_T of droplets of maximum radius R_T in the inhomogeneous case. The striking observation is that the largest droplets grow much faster on the inhomogeneous model than on either the homogeneous or adiabatic models even though, in the latter case, the liquid water content is about twice as great. For example, we see that about 150 seconds are required on the inhomogeneous model for the largest drops to achieve a radius of 13 μm, while about 400 to 500 seconds respectively are required on the adiabatic and homogeneous models. For $R = 15\,\mu$m the figures are about 200 seconds for the inhomogeneous model, 700 seconds on the adiabatic model and 800 seconds on the homogeneous. We see that on our inhomogeneous description of the entrainment process the largest droplets move through the condensational stage about three times as fast as is predicted classically. For larger values of $1/\lambda_0$ the rate of growth of the largest particles is not so great, as illustrated in Table (4), but even for large intervals between successive blobs ($\lambda_0^{-1} = 200, 300$ s) the rate of growth is about twice the classical (homogeneous) value. Telford and Chai (1980) have reached similar conclusions from a related description of the effects of entrainment upon the mixing process.

The principal conclusions presented in this section were found to be insensitive to variations in N, U, $T(o)$ and μ, and also to the choice of CCN activity spectrum and expression for λ.

TABLE 4. VALUES OF SUPERSATURATION (S_I); RADIUS (R_I) AND CONCENTRATION (N_T) OF THE LARGEST DROPS IN THE SPECTRUM, AND THE CONCENTRATION OF DROPLETS (ΔN) REMOVED AFTER 1000 m OF ASCENT, PREDICTED ON THE INHOMOGENEOUS MODEL FOR VARIOUS VALUES OF INITIAL FREQUENCY OF INFILTRATION (λ_0)

$U = 1\,\mathrm{m\,s^{-1}}$, $T(o) - 15°\mathrm{C}$, $N = 200\,\mathrm{cm^{-3}}$, $n = 38$, $\mu = 10^{-3}\,\mathrm{m^{-1}}$

λ^{-1} (s)	S_I (%)	R_I (μm)	N_T (1^{-1})	ΔN ($\mathrm{cm^{-3}}$)
10	0·34	26·1	0·15	3100
30	0·22	24·5	26	1300
100	0·14	21·0	47	400
300	0·12	20·0	76	210

5. DISCUSSION

The prediction, advanced in the preceding section, that inhomogeneous mixing can cause a small fraction of the droplets in a cloud to grow much more rapidly through their condensational stage, appears to offer a solution to the long-standing question, referred to in the Introduction, of the rate at which raindrops can be produced in cumulus. The agreement between the curves (W) and (I) in Figs. 7 and 8 suggests that values of $1/\lambda_0 \sim 10\,\mathrm{s}$ may be realistic in general, for cumulus clouds, and it is seen from Table 4 that the rate of growth is particularly high for such small blob-intervals. In this connection it is interesting to note that the values of N_T (about one per litre) presented in Table 3 are of the right order of magnitude for raindrop concentrations.

The reason for the greatly enhanced growth-rates on the inhomogeneous model is apparent from the inspection of Table 3 – the values of supersaturation are much greater. This is because, on the inhomogeneous model, more droplets are completely evaporated, and the newly activated ones that replace them cannot compete so effectively for the available water vapour. Thus the supersaturation rises above that for the homogeneous case, and those drops unaffected by the infiltrating blob will grow faster.

As shown in Table 4 the number of droplets ΔN that are replaced by CCN (subsequently activated) increases with initial blob frequency $1/\lambda_0$. For $\lambda_0{}^{-1} = 10\,\mathrm{s}$, when the spectral evolution predicted on the inhomogeneous model agrees particularly well with the observations of Warner (1969a), the number of droplets that have been replaced in 1 km of ascent is about 10 times the droplet concentration ($300\,\mathrm{cm^{-3}}$), which remains constant throughout this period. Thus only a very small fraction of those droplets initially formed by condensation at cloud base retain their identities during the ascent of the cloudy air to the 1 km level. Possible implications of this prediction with respect to cloud chemistry are currently being examined.

The extent to which the predicted spectral shapes and evolution, together with the rate of formation of embryonic raindrops, agree with observation provides encouragement for the idea that the mixing process in cumulus clouds is highly inhomogeneous. In paper II of this series field experiments are described which reinforce this viewpoint. To proceed further along these lines it is clearly necessary to take detailed account of the various time-constants, concerned with mixing and evaporation, which feature in the process of spectral evolution in an entraining cloud. At present we are exploring the feasibility of a stochastic

approach, in which turbulent eddies or blobs of both cloudy and undersaturated air, and existing on all relevant spatial scales, meet and intermingle on a random basis. When the vapour-deficit in an undersaturated blob exceeds the liquid water content in a blob of cloud with which it mixes evaporation will be total, provided that the droplets have time to evaporate before the ensemble mixes with its environment. In this situation the mixing process is equivalent to the extreme inhomogeneous case, utilized in our calculations. When these conditions are not met, partial evaporation will occur, and various time constants will have to be incorporated explicitly into the calculations. It appears that for the majority of combinations of eddy sizes these conditions will be met, at least to a first approximation; which is consistent with the finding that the extreme model of inhomogeneous mixing presented in this paper predicts spectra in reasonable agreement with those observed.

Acknowledgments

This research has been supported by the Natural Environment Research Council, the US Office of Naval Research and the Universities Space Research Association. We are grateful to Dr J. Warner for detailed and constructive comments on this work, as it evolved, and to Dr S. F. Darlow and Mrs S. E. A. Middleton for assistance with the computations.

References

Baker, M. B. and Latham, J. 1979 The evolution of droplet spectra and the rate of production of embryonic raindrops in small cumulus clouds, *J. Atmos. Sci.*, **36**, 1612–1615.

Bartlett, J. T. and Jonas, P. R. 1972 On the dispersion of the sizes of droplets growing by condensation in turbulent clouds, *Quart. J. R. Met. Soc.*, **98**, 150–164.

Corbin, R. G., Latham, J., Mill, C. S., Smith, M. H. and Stromberg, I. M. 1977 Inhomogeneities in the water properties of fogs and clouds, *Nature*, **267**, 32–33.

Corbin, R. G., Latham, J., Mill, C. S. and Stromberg, I. M. 1978 An assessment of the Keily Probe for the ground based measurement of drop size distributions in clouds, *Quart. J. R. Met. Soc.*, **104**, 729–736.

Corbin, R. G. 1979 Ph.D. thesis, Univ. Manchester.

Fukuta, N. and Walter, L. A. 1970 Kinetics of hydrometeor growth from a vapour-spherical model, *J. Atmos. Sci.*, **27**, 1160–1172.

Jonas, P. R. and Goldsmith, P. 1972 The collection efficiencies of small droplets falling through a sheared air flow, *J. Fluid Mech.*, **52**, 593–608.

Jonas, P. R. and Mason, B. J. 1974 The evolution of droplet spectra by condensation and coalescence in cumulus clouds, *Quart. J. R. Met. Soc.*, **100**, 286–295.

Knollenberg, R. G. 1976 Three new instruments for cloud physics measurements: the 2-D spectrometer, the Forward Scattering Spectrometer Probe, and the Active Aerosol Spectrometer, *Proc. Int. Conf. Cloud Physics*, Boulder, 554.

Latham, J. and Reed, R. L. 1977 Laboratory studies of the effects of mixing on the evolution of cloud droplet spectra, *Quart. J. R. Met. Soc.*, **103**, 297–306.

Lee, I. Y. and Pruppacher, H. R.	1977	A comparative study of the growth of cloud drops by condensation using an air parcel model with and without entrainment, *Pageoph.*, **115**, 523–545.
Mason, B. J.	1975	Discussion of Mason and Jonas' model of droplet growth in cumulus clouds by J. Warner. Reply, *Quart. J. R. Met. Soc.*, **101**, 178.
Mason, B. J. and Jonas, P. R.	1974	The evolution of droplet spectra and large droplets by condensation in cumulus clouds, *Ibid.*, **100**, 23–38.
May, K. R.	1949	An improved spinning top homogeneous spray apparatus, *J. Appl. Phys.*, **20**, 932–938.
Rodi, A. R.	1978	Small scale variability of the cloud droplet spectrum in cumulus clouds, *Proc. AMS Conf. Cloud Phys., Atmos. Elect.*, Issaquah, 88.
Telford, J. T. and Chai, S.	1980	A new aspect of condensation theory, *Pageoph.* (accepted).
Warner, J.	1969a	The microstructure of cumulus cloud. Pt. I, General features of the droplet spectrum, *J. Atmos. Sci.*, **26**, 1049–1059.
	1969b	The microstructure of cumulus cloud. Pt. II. The effect on droplet size distribution of the cloud nucleus spectrum and updraft velocity, *Ibid.*, **26**, 1272–1282.
	1970	The microstructure of cumulus cloud. Pt. III. The nature of the updraft, *Ibid.*, **27**, 682–688.
	1973a	The microstructure of cumulus cloud. Pt. IV, The effect on the droplet spectrum of mixing between cloud and environment, *Ibid.*, **30**, 256–261.
	1973b	The microstructure of cumulus cloud. Pt. V. Changes in droplet size distribution with cloud age, *Ibid.*, **30**, 1724–1726.
	1975	Discussion of Mason and Jonas's model of droplet growth in cumulus clouds, *Quart. J. R. Met. Soc.*, **101**, 176.